Journal of the Serbian Chemical Society
JSCS-info@shd.org.rs • www.shd.org.rs/JSCS
J. Serb. Chem. Soc. 85 (10) 1345–1356 (2020)
JSCS–5379
UDC 546.284–31SBA-15:544.362+
544.004.12:546.28'62
Original scientific paper

Investigation the effects of Al-grafting and calcination temperature on the acidity and physicochemical properties of silica SBA-15

REZA OROUJ, MEHDI RASHIDZADEH*, AKBAR IRANDOUKHT and SEPEHR SADIGHI

Catalysis Technologies Development Division, Research Institute of the Petroleum Industry, P. O. Box 14665-137, Tehran, Iran

(Received 20 November 2019, revised 6 April, accepted 14 April 2020)

Abstract: In this study, the effect of calcination temperature and Si/Al mole ratio on acidity and physicochemical properties of silica SBA-15 were investigated. Silica SBA-15 samples were calcined at 350, 450 and 550 °C, and then post-synthesis, the Al-grafting method was applied to incorporate aluminum species into their framework with Si/Al mole ratio of 10 and 30. Characterizations using small angle XRD and N_2 adsorption–desorption techniques indicated that the hexagonal mesoporous structure was retained after performing Al-grafting even at the high aluminum loading. Moreover, FTIR results implied that the aluminum species were incorporated into the SBA-15 framework. NH_3-TPD results showed that by decreasing Si/Al mole ratio at all calcination temperatures, the number of weak acid sites increased in comparison to those of the pure SBA-15 samples. Additionally, the maximum total acidity of synthesized samples was observed at the calcination temperature of 450 °C with Si/Al mole ratio of 30.

Keywords: silica SBA-15; post-synthesis Al-grafting; acidity; physicochemical properties.

INTRODUCTION

Hydrotreating and hydrocracking processes are usually performed over bifunctional catalysts containing active metal sites for hydrogenation/dehydrogenation reactions, and acid sites for cracking hydrocarbons.[1] The catalytic performance of hydrotreating/hydrocracking catalysts can be modify by changing the nature of the active metals or the support. Hence, modification of the physicochemical properties of the support is still one of the preferred methods used for enhancing catalytic activity.[2] The activity of a catalyst strongly depends on the combination of textural, chemical and physical properties of the support. Pore

* Corresponding author. E-mail: rashidzadehm@ripi.ir
https://doi.org/10.2298/JSC191129021O

size is a momentous property since each catalytic system requires a unique pore size for optimal active metal loading, diffusion and selectivity. Furthermore, high surface area and large total pore volume usually enhance catalyst loading that increases the number of active metal sites and decreases the reaction time. Moreover, the ability to control the acidity of the catalyst enables manufacturers to design desirable acid sites for the sake of optimizing product selectivity, activity and stability in miscellaneous catalytic applications.[1–3]

In the past few years, many works have been devoted to the application of mesoporous SBA-15 as a support.[4–5] This material has high surface area, large pore volume and a uniform hexagonal array of cylindrical mesopores. However, its lower acidity in comparison to zeolites creates a limitation for using it as a support in hydroprocessing applications. In order to increase the acidity of SBA--15, attempts have been made to incorporate heteroatom into its structure by direct or post synthesis grafting methods. However, depending on the preparation procedure, samples exhibit different structural, textural and surface characteristics.[3,6] Moreover, it is reported that silanol groups on the internal wall surface of SBA-15 are favorable for aluminum incorporation. Depending on synthesis method and calcination temperature, the type and amount of silanol groups can be varied.[6–7]

To form the SBA-15 mesostructure, a vigorous acidic reaction condition is required, which is not suitable for directly incorporating aluminum into its framework. The direct synthesis of Al-SBA-15 is difficult, and is rarely stoichiometric. Additionally, it often demands fine-tuned synthesis conditions and complicated procedures.[8] From this viewpoint, the development of a simple post-synthesis method for aluminating mesoporous SBA-15 becomes the last option. One of the disadvantages of the post-synthesis method is the formation of oxides inside the mesopores that can partially or fully block them. Therefore, surface area, total pore volume, pore diameter and order of structure, especially at high aluminum loadings are reduced. Moreover, not all of the aluminum atoms introduced are located in tetrahedral coordination in which aluminum is covalently bound to four Si atoms *via* oxygen bridges.[8–9] Analysis performed using the ^{27}Al MAS NMR method proved that calcination treatment after the alumination of SBA-15 samples enhances the intensity of the peak of aluminum in tetrahedral coordination. Hence, more aluminum is incorporated into the SBA-15 framework.[10]

Luan *et al.* investigated the effect of using different aluminum sources including aluminum chloride and isopropoxide, and sodium aluminate during post-synthesis of SBA-15. The results confirmed that alumination using aqueous sodium aluminate was the most suitable method. The ^{27}Al MAS NMR spectra of Al-SBA-15 that had been synthesized by reacting SBA-15 with a sodium aluminate solution at an Si/Al ratio of 20 showed only aluminum in tetrahedral coordination. Thus, aluminum was incorporated into the siliceous framework of SBA-15

due to presence of Na^+ that balance the negative charges associated with the tetrahedral aluminum framework.[10] This result was in line with research previously performed by Gao *et al.*[9]

The current research seeks to investigate the simultaneous effects of Al--grafting and calcination temperature on the acidity of SBA-15. Consideration is given to: *i*) the effect of calcination temperature (*i.e.*, 350, 450 and 550 °C) and *ii*) the effect of Si/Al mole ratio on specifications of Al-SBA-15 samples (*i.e.*, 10 and 30).

EXPERIMENTAL

Sample preparation

Mesoporous SBA-15 with hexagonal *P6mm* structure was prepared according to a well-known procedure.[11,12] In this method, the tri-block copolymer Pluronic P123 (M_{av} = 5800, $EO_{20}PO_{70}EO_{20}$, Sigma–Aldrich) and tetraethyl orthosilicate (TEOS, Aldrich, 98 %) were used as a structure-directing agent and silica source, respectively. of Pluronic P123 (2.4 g) and of ammonium fluoride (0.027 g) were dissolved in 84 ml of HCl (1.3 M) using a magnetic stirrer at room temperature. Then, 5.17 g of TEOS was slowly added into the solution under vigorous stirring. The mixture was stirred at 18 °C for 20 h, and then aged at 130 °C for 48 h without stirring. After filtering the mixture, the remaining solid was dried at 70 °C for 12 h. Finally, the calcination process was performed in static air at 350, 450 or 550 °C for 5 h.

To obtain Al-grafted SBA-15 with a Si/Al mole ratio of 10 or 30 (theoretical content), the mesoporous silica SBA-15 was used as a precursor. Additionally, sodium aluminate ($NaAlO_2$, Sigma–Aldrich) was used for post-synthetic alumination. In grafting procedure, 0.5 g of calcined pure SBA-15 was stirred in 50 ml deionized water containing the appropriate amount of $NaAlO_2$ for 6 h. To eliminate the excess $NaAlO_2$, the filtered materials were washed with deionized water. After drying at the room temperature for 2 days, the SBA-15 products were calcined in static air at the same calcination temperatures (350, 450 and 550 °C) for 5 h. According to the calcination temperature (350, 450 or 550 °C) and the nominal Si/Al mole ratio (10 or 30), the prepared samples were labeled as SBA-*x*-(*y*).

Characterization techniques

Al-grafted samples were characterized using different techniques to study their physical properties and acidities. Small-angle XRD patterns (SAXS) were recorded on an X'Pert Pro MDP using monochromatic Cu radiation with a wavelength of 1.54 Å in the low angle region (0.6 to 5.0° in the 2θ scale). XRD patterns were recorded in the range of $3° \leq 2\theta \leq 90°$ employing a Philips PW1720 diffractometer using Cu$K\alpha$ radiation (λ = 1.5406 Å). The textural properties of the samples were characterized using a Belsorb Max instrument. Thus, 30–40 mg of a sample was degassed in the preparing station under a helium stream at 300 °C for 2 h, and then the device was switched to the analysis station to perform adsorption and desorption under liquid nitrogen at –196 °C. The surface area was calculated with the multipoint Brunauer–Emmett–Teller (BET) equation[13] with the linear region in the P/P_0 range of 0.05 to 0.2. The total pore volume was calculated from the maximum amount of nitrogen adsorbed at a P/P_0 of 0.99. The Barret–Joyner–Halenda (BJH) method[14] was used to determine the pore size distribution. The micropore area was estimated using the correlation of t-Harkins & Jura (*t*-plot method[15]). Moreover, the acidic properties of the prepared samples were determined by AutoChem 2900 (Micromeritics) automatic analyzer equipped with a TC detector. Before

NH_3 adsorption, the samples were pretreated *in situ* at 500 °C for 90 min under helium flow in order to remove water and other contaminants. The samples were then cooled to 150 °C and contacted with NH_3. The desorption step was performed in a helium stream (50 ml min^{-1}) with a heating rate of 10 °C min^{-1} up to 750 °C. The Fourier transform infrared (FTIR) spectra were obtained using a Bruker Vertex 70 infrared spectrometer. The KBr pellet technique was applied to collect infrared spectra of samples at room temperature. The results are reported between 400 and 4000 cm^{-1} with a resolution of 4 cm^{-1}.

RESULTS AND DISCUSSION

The SAXS patterns of the SBA-450-(*y*) samples are presented in Fig. 1, as examples, to analyze the effect of Al-loading on the structure of the samples. As can be seen, SBA-450-(*y*) samples display three well-resolved diffraction peaks, indexed as (100), (110) and (200) reflections. These samples possess highly ordered hexagonal (*P6mm*) symmetry and a well-ordered mesoporous structure. Compared to the pure SBA-450, the SAXS patterns of the SBA-450-10Al and SBA-450-30Al are modified on aluminum grafting, revealing a slight structural modification of the pure SBA-450 after Al-grafting. In the diffraction patterns of the SBA-450-(y) samples, reflections of SBA-450-10Al and SBA-450-30Al have higher intensity compared to the pure sample. Therefore, the degree of crystallinity is enhanced by aluminum grafting. Despite the higher content of aluminum, SBA-450-10Al sample has lower crystallinity than SBA-450-30Al one. This phenomenon is probably due to the formation of aluminum-oxide islands in the SBA-450-10Al sample, and the consequential decrease in the order of the structure. As a significant observation, the SAXS analysis confirmed that the corresponding values for all three reflections ((100), (110) and (200)) shift to the lower 2θ values for the SBA-450-10Al and SBA-450-30Al samples. The shifting these peaks to lower 2θ values could indicate tetrahedral coordination of aluminum in the silica SBA-15 framework, which was also concluded by Mouli *et al.*[10] and Luan *et al.*[16] using ^{27}Al MAS NMR. According to those studies, shifting of 2θ in SAXS diffraction patterns to lower values may be linked to the Al–O bond being

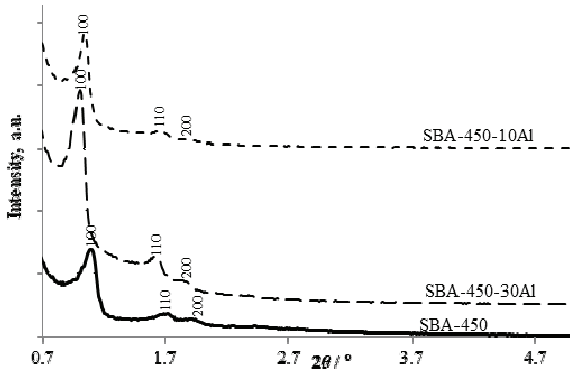

Fig. 1. SAXS patterns of the synthesize.00.d SBA-450-(*y*) samples.

longer than that of Si–O. Moreover, as seen from Fig. 1, the positions of the peaks in the SBA-450-10Al and SBA-450-30-Al samples are not significantly different. This observation indicates that these samples probably have the same size of the unit cell.

The XRD pattern of the SBA-450-10Al sample is presented in Fig. 2. As can be seen, the diffraction pattern of the SBA-450-10Al sample does not reveal the presence of any other crystalline phase, which is probably due to the high dispersion state of the metal oxide and/or its incorporation into the SBA-15 framework. It is supposed that the broad signal observed in this pattern at 2θ 15–35° corresponds to amorphous silica.

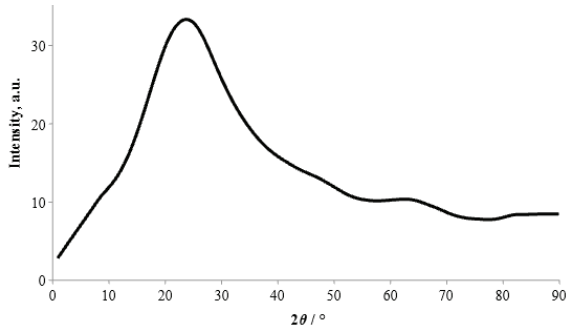

Fig. 2. Powder XRD pattern of the SBA-450-10Al sample.

The N_2 adsorption–desorption isotherms of the synthesized samples and their pore size distribution curves are shown in Fig. 3. The N_2 adsorption–desorption isotherm of the SBA-*x*-(*y*) samples shows the typical type IV curves with a type H1 hysteresis loop at a relative pressure P/P_0 around 0.7–0.8, which is a stunning evidence for well-ordered mesoporous materials. These curves show that the SBA-450-(*y*) and SBA-550-(*y*) samples have a narrow mono-modal pore size distribution centered on 10–11 nm. Conversely, pore size distribution of SBA-350-(*y*) samples is broader than those of other calcined samples.

In Fig. 3, it is demonstrated that the height of hysteresis decreases on increasing the aluminum content, which justifies the reduction in the amount of adsorbed gases after loading the aluminum. The cutback in the height of hysteresis loop is more discernible for the SBA-x-10Al samples. Furthermore, after Al-grafting, no significant variation in the hysteresis loop was perceptible, verifying the preservation of the arrangement of the pores in those samples. Moreover, the N_2 adsorption–desorption isotherms of the SBA-*x*-(*y*) samples exhibits a reduction in the capillary condensation step of the Al-containing samples, probably due to the filling of their pores by Al oxide species.

The values of key physical parameters of synthesized samples are listed in Table I. As seen, based on a previous study,[17] by adding inorganic NH_4F salt and

applying a low aging temperature, the mean pore diameter of samples increased in comparison to the sample synthesized using the Zhao *et al*. method.[11,12]

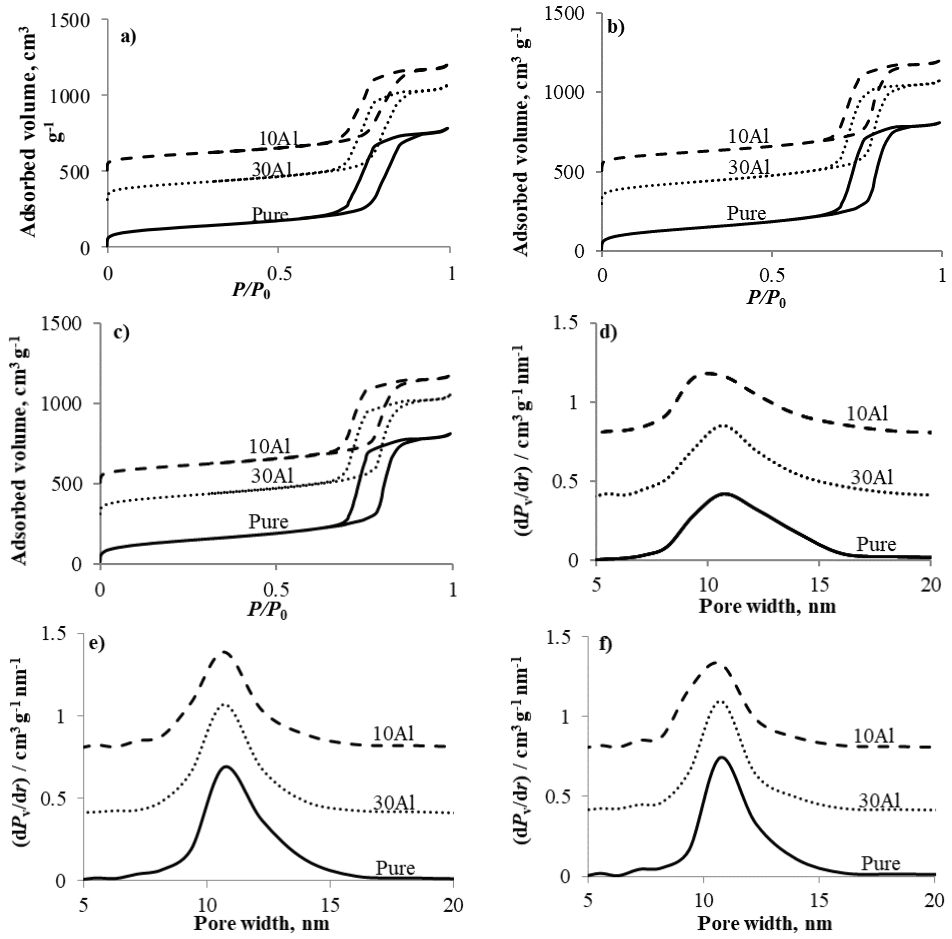

Fig. 3. N_2 adsorption–desorption isotherms of: a) SBA-350-(*y*), b) SBA-450-(*y*) and c) SBA-550-(*y*), and pore size distribution of: d) SBA-350-(*y*), e) SBA-450-(*y*) and f) SBA-550-(*y*) samples. The curves corresponding to SBA-*x*-10Al and SBA-*x*-30Al adsorption–desorption isotherms are offset by 500 and 300 $cm^3\ g^{-1}$ for clarity, respectively. The pore size distribution curves of SBA-*x*-10Al and SBA-*x*-30Al are shifted to 0.8 and 0.4, respectively.

Moreover, Table I shows that the BET surface areas and total pore volumes of the SBA-*x*-(*y*) samples decrease due to the probability of the formation of Al_2O_3 islands and the blockage of some pores after incorporation of aluminum into the pure SBA-*x* samples. For samples calcined at 550 °C, the reduction in the surface area was more pronounced however, this abatement (about 20 % at a

Si/Al mole ratio of 10) was lower than the value reported by Luan *et al.* (about 42 % reduction in surface area after the loading of aluminum at a Si/Al mole ratio of 20).[10] Gurinov *et al.* concluded that significant reduction in the surface area and total pore volume of Al-grafted samples was due to a gradual filling of the rough mesoporous walls instead of the formation of a homogenous aluminum film.[18] The BJH pore diameters of the SBA-*x*-(*y*) samples exhibited a different trend at the same Si/Al mole ratio and did not substantially vary after Al-grafting.

TABLE I. Textural characteristics of synthesized samples

Sample	BET surface area, $m^2 g^{-1}$	Micropore area, $m^2 g^{-1}$	Total pore volume, $cm^3 g^{-1}$	Average pore diameter, nm	
				BJH adsorption	BJH desorption
SBA-350	439	65	1.20	11.73	8.76
SBA-350-10Al	385	33	1.08	11.30	8.86
SBA-350-30Al	409	39	1.17	11.48	9.06
SBA-450	478	27	1.25	11.08	8.85
SBA-450-10Al	412	22	1.08	10.89	8.54
SBA-450-30Al	443	29	1.19	10.76	8.62
SBA-550	497	30	1.25	11.02	8.79
SBA-550-10Al	401	26	1.04	10.59	8.29
SBA-550-30Al	442	26	1.17	10.83	8.49

The pure SBA-450 and SBA-550 samples had the same specific surface area and total pore volume whereas pure SBA-350 sample had the lowest surface area because remaining some amount of the P123 surfactant remained in its framework even after calcination at 350 °C.

The FTIR spectrums recorded in the range of 400–4000 cm^{-1} for SBA-450-(*y*) samples are presented in Fig. 4. These figures show four major peaks at 3200–3600, 1000–1250, 800 and 400–500 cm^{-1}. All samples exhibit broad band at 1000–1250 cm^{-1} due to asymmetric Si–O–Si stretching modes (Q^4 sites). The bands around 800 and 960 cm^{-1} are related to T–O (T = Si or Al) symmetric

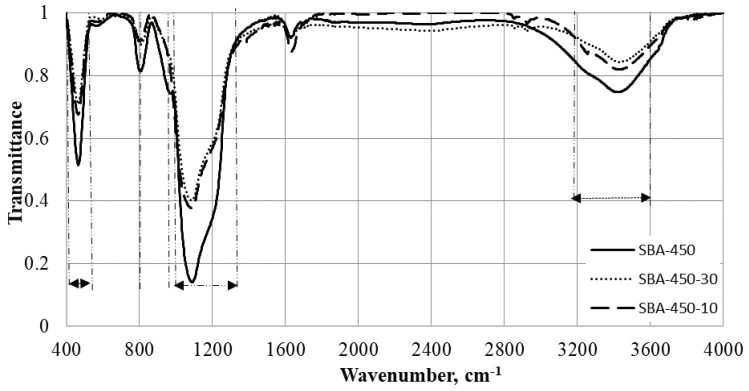

Fig. 4. FTIR spectra of SBA-450-(y) samples.

stretching mode, and their intensities decrease after incorporation of aluminum into pure SBA-450 framework. Moreover, the band at 400–500 cm^{-1} is assigned to the Si–O bending vibration. The broad band at 3200–3600 cm^{-1} can be attributed to O–H stretching of Si–OH silanol groups (Q^2 and Q^3 sites) and Brønsted acid sites. The intensity of the 1000–1250 and 3200–3600 cm^{-1} peaks are smaller in the SBA-450-10Al and SBA-450-30Al samples than those of pure SBA-450, demonstrating a lower density of surface Si–O–Si and Si–OH in the former samples. These results are in agreement with the results of Mouli *et al*. that the number of Q^4 sites decreases on Al-grafting in the SBA-15 framework.[16]

It is well-known that the acidity of a catalyst strongly affects catalytic reactions. To determine the acidity of the samples, NH_3 temperature programmed desorption (NH_3-TPD) measurements were performed. Ammonia is a basic molecule and it is strongly adsorbed by acidic sites. It is obvious that the greater is the strength of an acidic site, the higher is the desorption temperature. For the SBA-*x*-(*y*) samples, NH_3-TPD characterization results are displayed in Figs. 5 and 6, and also given in Table II. As shown, the NH_3-TPD profile for all SBA-*x*-(*y*) samples has two peaks. The first peak from 102 to 214 °C corresponds to weak acidity (mainly contributed by pentahedral aluminum species and surface hydroxyl group attached to Si or Al), and the second from 665 to 738 °C is attributed to strong acid sites (tetrahedral aluminum species and isolated silanols).[18,19] By increasing aluminum content of samples for all studied calcination temperatures, the position of the peak attributed to the weak acidity is shifted to the higher value while irregular variation is observed in the strong acid peaks.

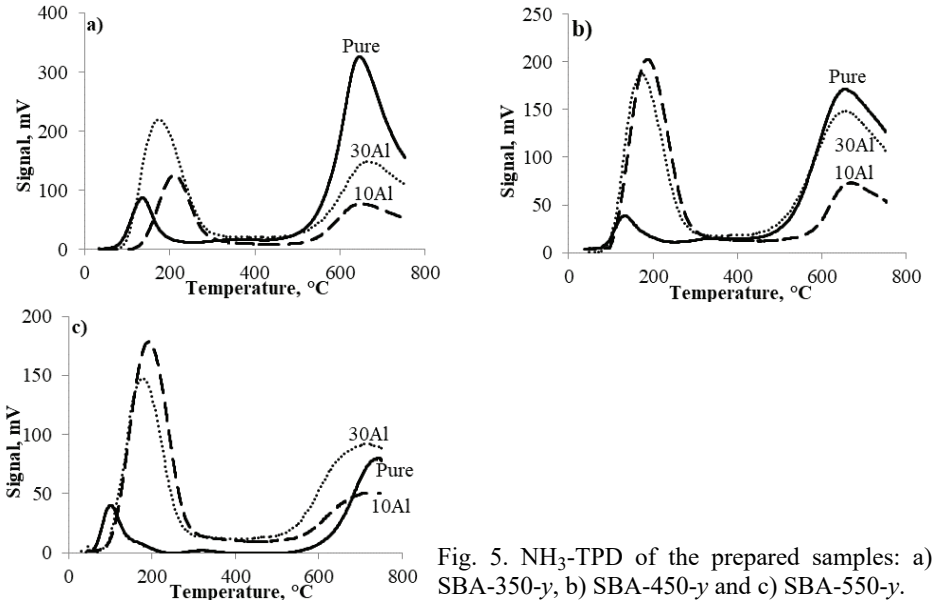

Fig. 5. NH_3-TPD of the prepared samples: a) SBA-350-*y*, b) SBA-450-*y* and c) SBA-550-*y*.

The pure SBA-*x* samples (see Table II and Fig. 5) have a smaller number of weak acid sites; intense peaks of the strong acid sites are augmented in these samples. Aluminum grafting for samples calcined at 450 and 550 °C enhances the total number of acid sites but strong acid sites are partially diminished. Therefore, the pure SBA-*x* samples have more strong acid sites than the SBA-*x*--10Al and SBA-*x*-30Al ones. Intensification of the weak acid sites with increasing aluminum content is attributed to the presence of Brønsted acid sites and the availability of aluminum species in pentahedral coordination.

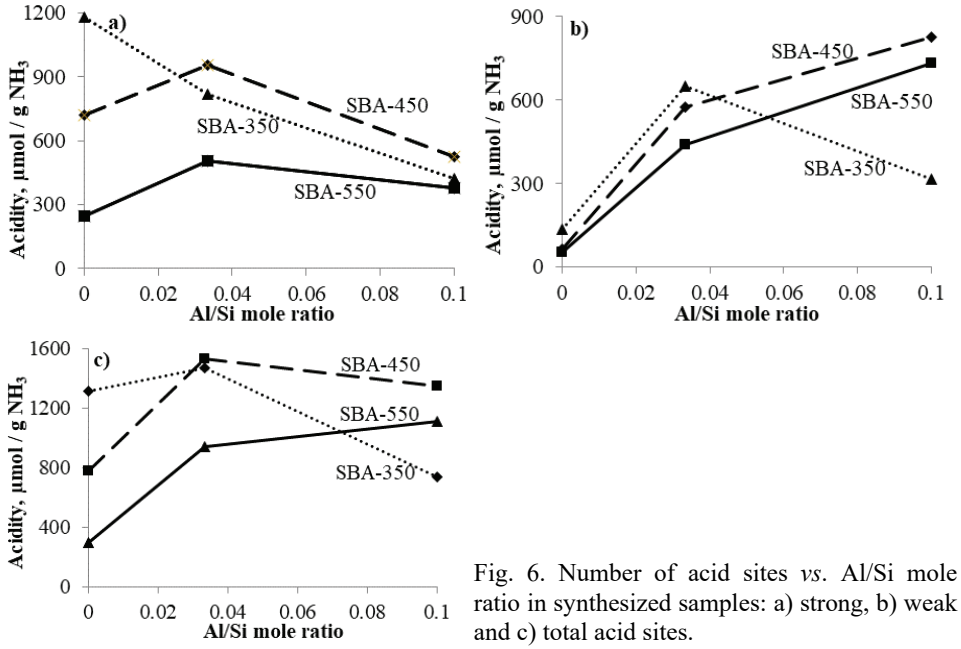

Fig. 6. Number of acid sites *vs*. Al/Si mole ratio in synthesized samples: a) strong, b) weak and c) total acid sites.

TABLE II. Nature and amount of acid sites in the SBA-*x*-(*y*) samples prepared at different calcination temperatures and Si/Al mole ratios

Sample	Amount of acid sites, μmol g^{-1} NH_3 (peak temperature, °C)		
	Weak	Strong	Total
SBA-350	137 (134)	1180 (665)	1317
SBA-350-10Al	316 (214)	423 (678)	739
SBA-350-30Al	650 (182)	819 (684)	1469
SBA-450	62 (146)	720 (678)	782
SBA-450-10Al	827 (190)	523 (699)	1350
SBA-450-30Al	573 (178)	956 (672)	1529
SBA-550	52 (102)	248 (738)	300
SBA-550-10Al	731 (193)	378 (703)	1109
SBA-550-30Al	441 (179)	504 (697)	945

The acidity of the Al-grafted samples varied even at high aluminum content but there was no significant variation in physical and structural properties of these samples. The main reason for this phenomenon is the facilitated diffusion of aluminum precursor to the mesochannels of pure SBA-x particles during Al--grafting.

As seen in Fig. 6 and Table II, the acidity of samples was adjusted by varying the calcination temperature and Al/Si mole ratio.

Since aluminum in its tetrahedral and pentahedral coordination forms acidic sites, an increase in the amount of aluminum higher than Al/Si mole ratio of 0.033 establishes aluminum oxides in octahedral coordination. It is believed that these extra aluminum species do not affect the acidity. Moreover, aluminum oxide islands are created by increasing aluminum; therefore, total acidity of samples is reduced due to overlapping acidic sites.

Furthermore, Fig. 6 shows that calcination at 450 °C with Al/Si mole ratio of 0.033 is recommended for catalysts requiring high number of acid sites. On increasing the calcination temperature from 450 to 550 °C, the acidity of the samples decreased due to condensation of silanol group, enabling an anchor for aluminum compounds.

CONCLUSIONS

In this research, the effects of the calcination temperature and aluminum grafting on the acidity and physical properties of SBA-15 were investigated. The results obtained from SAXS, FTIR and NH_3-TPD techniques proved the incorporation of aluminum into the SBA-15 framework. Although the values for all three reflections (100, 110 and 200) shifted to lower 2θ value, the SAXS results illustrated that the structural order of SBA-*x*-(*y*) samples was maintained after grafting aluminum. The pore size distribution curves indicated that SBA-450-(*y*) and SBA-550-(*y*) samples had a narrow mono-modal pore size distribution even after grafting aluminum in high amounts. Furthermore, the specific surface area and total pore volume showed a maximum reduction of 20 and 17 %, respectively at a Si/Al mole ratio of 10. The NH_3-TPD results showed that the maximum number of acid sites was achievable at a Si/Al mole ratio of 30, and loss of total acidity was observed by increasing aluminum content due to the appearance of octahedral aluminum species and formation of aluminum islands. In addition, the total acidity decreased on increasing the calcination temperature. It should be mentioned that strong acid sites were dominant in pure SBA-*x* samples while in aluminum grafted samples the weak ones were assertive.

Acknowledgement. The Catalysis Technologies Development Division of The Research Institute of the Petroleum Industry is gratefully acknowledged for financial support (Project No. 83990061).

ИЗВОД

ИСПИТИВАЊЕ УТИЦАЈА МОДИФИКАЦИЈЕ ЈОНСКИМ ВРСТАМА АЛУМИНИЈУМА И ТЕМПЕРАТУРЕ КАЛЦИНАЦИЈЕ НА КИСЕЛОСТ И ФИЗИЧКО–ХЕМИЈСКА СВОЈСТВА SiO_2 SBA-15

REZA OROUJ, MEHDI RASHIDZADEH, AKBAR IRANDOUKHT, SEPEHR SADIGHI

Catalysis Technologies Development Division, Research Institute of the Petroleum Industry, Tehran, Iran

У овом раду је испитиван утицај температуре калцинације и односа Si/Al на киселост и физичко–хемијска својства SiO_2 SBA-15. Узорци SiO_2 SBA-15 су калцинисани на 350, 450 и 550 °C, након чега су модификовани јонским врстама алуминијума, при молским односима Si/Al од 10 и 30, да би се ове врсте инкорпорирале у структуру SBA-15. Карактеризација применом рендгенске дифракције на малим угловима и N_2 адсорпције–десорције је указала да се хексагонална мезопорозна структура задржава и након модификације Al-врстама, чак и при великом садржају алуминијума. Додатно, резултати FTIR анализе указују на могуће инкорпорирање Al-врста у структуру SBA-15. Резултати температурно програмиране десорпције амонијака (NH_3-TPD) су показали да се при смањењу односа Si/Al на свим температурама калцинације повећава број слабо киселих места у односу на чист SBA-15. Додатно, максимална вредност укупне киселости је постигнута при температури калцинације 450 °C и при молском односу Si/Al од 30.

(Примљено 20. новембра 2019, ревидирано 6. априла, прихваћено 14. априла 2020)

REFERENCES

1. J. C. Morales-Ortuno, R. A. Ortega-Domínguez, P. Hernández-Hipólito, X. Bokhimi, T. E. Klimova, *Catal. Today* **271** (2016) 127 (https://doi.org/10.1016/j.cattod.2015.07.028)
2. K. Jaroszewska, A. Masalska, D. Czycz, J. Grzechowiak, *Fuel Process. Technol.* **167** (2017) 1 (https://doi.org/10.1016/j.fuproc.2017.06.012)
3. T. Klimova, J. Reyes, O. Gutierrez, L. Lizama, *Appl. Catal., A* **335** (2008) 159 (https://doi.org/10.1016/j.apcata.2007.11.008)
4. Y. Ganjkhanlou, Z. Tišler, J. M. Hidalgo, K. Frolich, J. Kotera, P. Čičmanec, R. Bulanek, *Chem. Pap.* **72** (2018) 937 (https://doi.org/10.1007/s11696-017-0336-z)
5. Gh. Mohammadi Ziarani, M. Rahimifard, F. Nouri, A. Badiei*, J. Serb. Chem. Soc.* **80** (2015) 1265 (https://doi.org/10.2298/JSC140930045M)
6. J. M. Rosenholm, T. Czuryszkiewicz, F. Kleitz, J. B. Rosenholm, M. Linde, *Langmuir* **23** (2007) 4315 (https://doi.org/10.1021/la062450w)
7. R. Ojeda-López, I. J. Pérez-Hermosillo, J. M. Esparza-Schul, A. Cervantes-Uribe, *Adsorption* **21** (2015) 659 (https://doi.org/10.1007/s10450-015-9716-2)
8. H. M. Kao, Ch. Ch. Ting, Sh. W. Chao, *J. Mol. Catal., A: Chem.* **235** (2005) 200 (https://doi.org/10.1016/j.molcata.2005.03.026)
9. D. Gao, A. Duan, X. Zhang, Zh. Zhao, E. Hong, J. Li, H. Wang, *Appl. Catal., B* **165** (2015) 269 (https://doi.org/10.1016/j.apcatb.2014.10.034)
10. Zh. Luan, M. Hartmann, D. Zhao, W. Zhou, L. Kevan, *Chem. Mater.* **11** (1999) 1621 (https://doi.org/10.1021/cm9900756)
11. D. Zhao, J. Feng, Q. Huo, N. Melosh, G. H. Fredrickson, B. F. Chmelka, G. D. Stucky, *Science* **279** (1998) 548 (https://doi.org/10.1126/science.279.5350.548)
12. D. Zhao, Q. Huo, J. Feng, B. F. Chmelka, G. D. Stucky, *J. Am. Chem. Soc.* **120** (1998) 6024 (https://doi.org/10.1021/ja974025i)
13. S. Brunauer,P. H. Emmett, E. Teller, *J. Am. Chem. Soc.* **60** (1938) 309
14. E. P. Barrett, L. G. Joyner, P. P. Halenda, *J. Am. Chem. Soc.* **73** (1951) 373

15. W. D. Harkins, G. J. Jura, *Chem. Phys.* **11** (1943) 430
16. K. Ch. Mouli, K. Soni, A. Dalai, J. Adjaye, *Appl. Catal., A: Gen.* **404** (2011) 21 (https://doi.org/10.1016/j.apcata.2011.07.001)
17. R. Orouj, M. Rashidzadeh, A. Irandokht, S. Sadighi, *Energy Sources, A* (2019) (https://doi.org/10.1080/15567036.2019.1655116)
18. A. A. Gurinov, Y. A. Rozhkova, A. Zukal, J. Cejka, I. G. Shenderovich, *Langmuir* **27** (2011) 12115 (https://doi.org/10.1021/la2017566)
19. G. Chandrasekar, M. Hartmann, M. Palanichamy, V. Murugesan, *Catal. Commun.* **8** (2007) 457 (https://doi.org/10.1016/j.catcom.2006.07.021).